

# Heparin binding to cobra basic phospholipase A<sub>2</sub> depends on heparin chain length and amino acid specificity

Yi-Hung Lin, Shao-Chen Lee, Payne Y. Chang, P.K. Rajan, Shih-Che Sue, Wen-guey Wu\*

Department of Life Sciences, National Tsing Hua University, Hsinchu 30043, Taiwan

Received 2 April 1999; received in revised form 30 May 1999

**Abstract** Heparin is shown to bind specifically to the carboxy-terminal region of toxic type I phospholipase A<sub>2</sub> from *Naja nigricollis* (N-PLA<sub>2</sub>) by competition assay using synthetic polypeptides and heparin affinity chromatography. The binding strength is seen to depend on heparin chain length and the presence of *N*-sulfate groups of heparin. It is observed that both electrostatic and non-electrostatic interactions are involved in the specific binding of heparin to the carboxy-terminus. When heparin's size is at least a decasaccharide, about two molecules of N-PLA<sub>2</sub> bind to one molecule of heparin, as evidenced by the chemical estimate of protein to carbohydrate ratio in such N-PLA<sub>2</sub>/heparin complexes. Based on such a stoichiometric measurement and computer modeling of the N-PLA<sub>2</sub>/heparin complex, it is suggested that the binding sites of the two N-PLA<sub>2</sub> molecules on one heparin molecule lie on the opposite sides of the heparin chain.

© 1999 Federation of European Biochemical Societies.

**Key words:** Phospholipase A<sub>2</sub>; Heparin; Glycosaminoglycan

## 1. Introduction

Phospholipases A<sub>2</sub> (PLA<sub>2</sub>s), which catalyze the hydrolysis of phospholipids at the *sn*-2 acyl chain and generate free fatty acids and lysophospholipids, are involved in a variety of physiological functions [1]. Mammalian secretory PLA<sub>2</sub> including human PLA<sub>2</sub> (hIIa PLA<sub>2</sub>) are suggested to be associated with the inflammatory host-defense process [2]. On the other hand, snake venom PLA<sub>2</sub> causes tissue necrosis of the bitten victim to exert its toxicity [3]. Glycosaminoglycans (GAGs) found on the outer membrane of the cell, among which heparins have the highest structural diversity and sulfate content, are proposed to play important roles in regulating the enzymatic or pharmacological action of these secretory class I and II PLA<sub>2</sub>s [4]. It is suggested that the biological activities of these heparin binding enzymes depend on whether proper and timely presentation of these molecules could occur via their binding to GAG molecules near the cell surface.

The heparin binding sites of different PLA<sub>2</sub>s from snake venom have been assigned to be located at either the carboxy- or amino-terminal region based on their sequence homology and on whether heparin can inhibit their enzymatic activity [5]. In most of these cases, the interactions of PLA<sub>2</sub> with heparin are electrostatic in nature, originating from the high negative charge density of heparin. However, it is not known whether non-electrostatic interactions between PLA<sub>2</sub> and heparin molecules are also involved as in the case of other hep-

arin binding proteins such as fibroblast growth factor and cobra cardiotoxins [6,7].

In the present study we investigate the nature of interaction of N-PLA<sub>2</sub>, a basic PLA<sub>2</sub> from *Naja nigricollis*, with heparin and address the issue of the possible heparin chain length dependence and the role of the presence of *N*-sulfate groups in heparin on such an interaction. We combined the peptide competition assay, enzymatic activity measurement, usage of different chain length and de-*N*-sulfated heparin molecules, computer modeling and other methods to obtain a clear understanding of the above.

## 2. Materials and methods

### 2.1. Materials

Heparins with different molecular weights were purchased from Sigma. Crude venom from *Naja atra*, *Naja nigricollis* and *Naja mosambica* were also from Sigma. All PLA<sub>2</sub>s listed in Table 1 were purified from crude venom by chromatography using SP-Sephadex C-25, followed by reverse phase HPLC as described with modification [8,9]. The assignments of these PLA<sub>2</sub>s were done by amino acid composition analysis, in combination with enzymatic activity measurement [10].

Four polypeptides with amino acid sequences corresponding to residues 51–57 (-YEKAGKM-), 63–69 (-LTLYKYYK-), 111–117 (-NINFKKR-), and 111–119 (-NINFKKRCQ-) of N-PLA<sub>2</sub> molecules and three other peptides with scramble, inverse and modified sequences of the intrinsic peptide 111–117, namely -NKNFQIRC-, -QCRKKFNIN- and -NINFKKRCA-, respectively, were synthesized by Genosys Biotech. Inc. using a segmented synthesis process [11].

### 2.2. Immobilized heparin binding assay

The effective NaCl and polypeptide concentrations required to dissociate the N-PLA<sub>2</sub>/heparin complex were determined using a heparin-Sepharose column (HiTrap, 1 ml, Pharmacia), fitted to a Bio-Rad FPLC system [10] and a batch-type competition binding assay, respectively. The latter was performed by incubating N-PLA<sub>2</sub> (typically 40 μM) along with the desired concentrations of the synthetic polypeptides and heparin gel (10 μl of swollen Sepharose gel with 1 μg of coupled heparin) pre-equilibrated with the binding buffer (10 mM Tris-HCl, pH 8.0, 100 mM NaCl, and 0.02% NaN<sub>3</sub>). After 2 h of incubation at room temperature, the reaction mixtures were centrifuged. The amount of eluted N-PLA<sub>2</sub> was quantified by an enzymatic method using the standard activity curve of N-PLA<sub>2</sub> at various concentrations.

### 2.3. Enzyme depolymerization of heparin

Typically, 100 mg of porcine intestinal mucosal heparin was depolymerized by 40 mIU *Flavobacterium* heparinase I (Sigma H-2519) in a 1 ml reaction buffer as described previously [12]. Average molecular weights and the corresponding carbohydrate chain lengths were estimated from gradient polyacrylamide gel electrophoresis [13]. The molecular weight and compositions of depolymerized GAGs (dpGAGs), ranging from a disaccharide to a decasaccharide, were characterized by mass spectrometry and 2-D NMR spectroscopy (COSY and NOESY), respectively as described [14,15]. Other than dpGAGs, heparin of low molecular weight (LMW-heparin, MW ~ 3000) with average chain length greater than a decasaccharide is also used in these studies.

\*Corresponding author. Fax: (886) (3) 5715934.  
E-mail: lswwg@life.nthu.edu.tw

Table 1

Correlation of amino acid sequences of PLA<sub>2</sub>s from Taiwan and African cobras and NaCl concentration required to dissociate the heparin-PLA<sub>2</sub> complex

	10	20	30	40	50	60
<b>A-PLA<sub>2</sub></b>	NLYQFKNMIQ	CTVPSRSWWD	FADYGCYCGR	GGSGTPVDDL	DRCCQVHDNC	YNEAEKISGC
<b>N-PLA<sub>2</sub></b>	NLYQFKNMIH	CTVPSRPWWH	FADYGCYCGR	GGKGTAVDDL	DRCCQVHDNC	YEKAGKM-GC
<b>M3-PLA<sub>2</sub></b>	NLYQFKNMIH	CTVPSRPWWH	FADYGCYCGR	GGKGTAVDDL	DRCCQVHDNC	YEKAGKM-GC
<b>M2-PLA<sub>2</sub></b>	NLYQFKNMIH	CTVPSRPWWH	FADYGCYCGR	GGKGTAVDDL	DRCCQVHDNC	YGEAEKL-GC
<b>M1-PLA<sub>2</sub></b>	NLYQFKNMIH	CTVPSRPWWH	FADYGCYCGR	GGKGTAVDDL	DRCCQVHDNC	YGEAEKL-GC
	<b>*I</b>					
	70	80	90	100	110	120
<b>WPYFKTYSYE</b>	CSQ-GTLTCK	GGNN-CAAAA	VCDCLRLAAI	CFAGAPYNDN	DYNINLKARC	<b>QE 130±20</b>
<b>WPYLTLYKYK</b>	CSQ-GKLTCS	GGNSKCGAA-	VCNCDLVAAN	CFAGARYIDA	NYNINFKKRC	<b>Q 570±20</b>
<b>WPYFTLYKYK</b>	CSQ-GKLTCS	GGNSKCGAA-	VCNCDLVAAN	CFAGARYIDA	NYNINFKKRC	<b>Q 490±20</b>
<b>WPYLTLYKYE</b>	CSQ-GKLTCS	GGNNKCAAA-	VCNCDLVAAN	CFAGARYIDA	NYNINLKERC	<b>Q 140±20</b>
<b>WPYLTLYKYE</b>	CSQ-GKLTCS	GGNNKCEAA-	VCNCDLVAAN	CFAGAPYIDA	NYNIDFKERC	<b>Q F.T.<sup>†</sup></b>
	<b>*II</b>			<b>*III</b>		

A-, N-, and M-PLA<sub>2</sub> denote PLA<sub>2</sub>s from *Naja atra*, *Naja nigricollis* and *Naja mossambica*, respectively, where M1, M2, and M3-PLA<sub>2</sub> are subdivisions of the same venom from *Naja mossambica*.

\*Potential heparin binding site.

@Salt concentration required to elute PLA<sub>2</sub> from the heparin affinity column.

#Flow-through (F.T.) of the heparin affinity column during the initial loading in 10 mM Tris. The deviation was estimated from the possible dead volume and the fraction volume during sample collection.

#### 2.4. Fluorescence experiments

8-Anilino-1-naphthalene sulfonate (ANS) was included in the N-PLA<sub>2</sub> containing solution to monitor the possible heparin-induced fluorescence changes of the ANS bound to N-PLA<sub>2</sub>. The excitation and emission wavelengths for ANS were set at 390 and 470 nm, respectively, on a SLM 4800 fluorescence spectrometer. To determine the dissociation constant ( $K_d$ ), computer simulation was performed based on the equation:  $K_d = ([H]_t - [P_nH])([P]_t - n[P_nH])/[P_nH]$ , where  $[P]$ ,  $[H]$  and  $[P_nH]$  represent the concentrations of PLA<sub>2</sub>, heparin and PLA<sub>2</sub>/heparin complex, respectively [5].

#### 2.5. Molecular modeling

Molecular modeling was conducted using Insight II on a SGI O2 workstation (Silicon Graphics, Inc.). A computer model of N-PLA<sub>2</sub> was constructed using the known crystal structure of PLA<sub>2</sub> from *Naja atra*, A-PLA<sub>2</sub> (~80% homology to N-PLA<sub>2</sub> based on the amino acid sequence) [16] as starting geometry. Simulations of heparin's binding to N-PLA<sub>2</sub> were performed through seven docking experiments, where heparin was initially docked near the charge cluster III (Table 1), i.e., around Lys-114, Lys-115 and Arg-116 in accordance with previous binding results. Molecular dynamics simulation with a time step of 1 fs was used to obtain the model of the N-PLA<sub>2</sub>/heparin complex after 10–40 ps. The non-bonded cutoff value was set at 15 Å. Energy minimization of the complex was finally performed to remove improper atom contacts and forces.

### 3. Results and discussion

#### 3.1. Heparin affinity chromatography

By determining the NaCl concentration required to elute different cobra PLA<sub>2</sub>s (listed in Table 1) from the heparin affinity column and correlating it with the amino acid sequences of homologous PLA<sub>2</sub> from Taiwan and African cobras, we could identify three potential amino acid positions involved in heparin binding (marked by asterisks in Table 1). They are near Lys-53, Lys-70, and Lys-118 (Table 1) and are classified here as positively charged clusters I, II, and III of cobra basic PLA<sub>2</sub>, respectively. It was observed that addition of LMW-heparin did not alter the enzymatic activity of

N-PLA<sub>2</sub> toward DMPC/Triton X-100 mixed micelles ( $K_m$  for N-PLA<sub>2</sub> is  $0.17 \pm 0.03$  and  $0.19 \pm 0.06$  mM without and with  $0.3 \mu\text{M}$  LMW-heparin, respectively) as well as its  $\text{Ca}^{2+}$ -dependent activity. Thus it appears that heparin binds to N-PLA<sub>2</sub> in locations far away from the enzymatic catalytic regions.

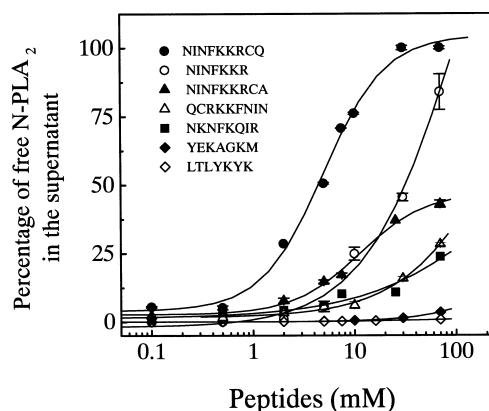


Fig. 1. Competition of binding between synthetic polypeptides and N-PLA<sub>2</sub> toward immobilized heparin. Polypeptides used here correspond to the indicated amino acid sequences derived from N-PLA<sub>2</sub>. Approximately 1  $\mu\text{g}$  of immobilized heparin was mixed with  $40 \mu\text{M}$  of N-PLA<sub>2</sub> and increasing amounts of polypeptides were added to a final volume of 120  $\mu\text{l}$  of binding buffer. The unbound N-PLA<sub>2</sub> that was released free in the supernatant was quantified by an enzymatic method using the standard activity curve of N-PLA<sub>2</sub> at various concentrations. (●) Peptide 110–118; (○) peptide 110–116; (▲) peptide 110–118 with Ala substituted for Gln; (△) inverse peptide of 110–118; (■) scramble peptide of 110–118; (◆) peptide 51–57; and (◇) peptide 63–69. Values are the mean of triplicate assays  $\pm$  S.D. If not shown, S.D. is smaller than the symbol size.

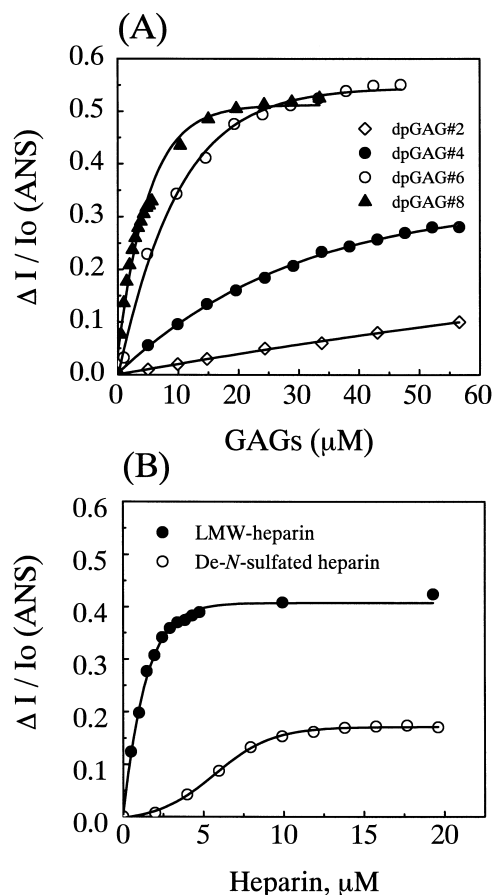


Fig. 2. Effect of using dpGAGs with different chain lengths on the binding with N-PLA<sub>2</sub>. dpGAG#*n* denotes a heparin chain of *n* saccharide units. A: Relative changes in ANS fluorescence intensity at the indicated chain lengths: (◇) dpGAG#2; (●) dpGAG#4; (○) dpGAG#6 and (▲) dpGAG#8. Fluorescence changes ( $\Delta I$ ) of the enzyme-bound ANS (60  $\mu M$ ) for 2  $\mu M$  N-PLA<sub>2</sub> in the presence of increasing quantities of dpGAGs were calculated from the average fluorescence intensities at 470 nm. Data were then analyzed by non-linear regression with a constraint of only one binding site. The  $K_d$  of N-PLA<sub>2</sub>/dpGAG complexes for dpGAG with chain length of #2, #4, #6, and #8 were found to be  $>100$ ,  $37 \pm 2$ ,  $8.1 \pm 0.7$ , and  $0.7 \pm 0.1$ , respectively. B: The N-sulfate group of heparin is involved in the binding as evidenced by the dependence of relative ANS fluorescence changes as a function of LMW-heparin (●) and de-N-sulfated heparin (○) concentration.

### 3.2. Polypeptide competition experiments

Fig. 1 shows the concentration of whole N-PLA<sub>2</sub> that is displaced into buffer due to the more favored binding of competing polypeptide to heparin. The peptide with its sequence corresponding to region III, i.e. 111–117 near the carboxy-terminus, exhibits significant competition with N-PLA<sub>2</sub>. This interaction is specific since hepta peptide 111–117 (open circle) competes quite favorably with N-PLA<sub>2</sub> whereas the other two hepta peptides 51–57 (region I) and 63–69 (region II) (closed and open diamonds) shows little ability to do so. Such specificity does not arise merely because of the presence of three positively charged amino acid residues in the peptide 111–117, compared to only two positively charged residues in 51–57 and 63–69. This is because the inclusion of two additional non-charged residues, i.e. Cys-Gln, at the carboxy-terminus increases the binding by almost one order of magnitude (com-

pare closed and open circles). Secondly, substitution of Gln by Ala (closed triangle) reduces its binding affinity by a similar amount, suggesting that the enhanced activity is not due to the potential oxidation of the introduced free Cys residues. Thirdly, the control peptides with reversed (open triangle) and scrambled (closed square) sequences derived from the intrinsic sequence (111–117) near the carboxy-terminus exhibit weaker binding than the intrinsic one itself. This is conclusive for the fact that heparin can indeed bind to the carboxy-terminus of N-PLA<sub>2</sub> via both electrostatic interaction and non-electrostatic interaction (probably by hydrogen bond formation) and this binding is quite specific to the sequence of the amino acids near the carboxy-terminus.

### 3.3. Heparin chain length and N-sulfation-dependent binding

Having identified the possible binding site of N-PLA<sub>2</sub> to heparin to be near the carboxy-terminus we looked for possible dependence of the binding on heparin's chain length. Fig. 2A shows a steady increase in the ANS fluorescence intensity with increasing dpGAG concentrations for different chain lengths, from a disaccharide to an octasaccharide. The  $K_d$  values for different dpGAG chain lengths indicate that dpGAG's binding strength can increase by about 50-fold when chain length varies from a tetrasaccharide to an octasaccharide. However, a heparin molecule with chain length of a tetrasaccharide can itself cover the binding site near the C-terminus of N-PLA<sub>2</sub>, implying that other regions of heparin should also participate in the binding.

Apart from heparin chain length, the presence of sulfate groups is also found to be important in a binding event of heparin with N-PLA<sub>2</sub>. As seen in Fig. 2B, binding strength of de-N-sulfated heparin to N-PLA<sub>2</sub> is markedly reduced as compared with the same for regular LMW-heparin. Thus the N-sulfate group of heparin must also be involved in an important manner in the specific interaction of heparin with N-PLA<sub>2</sub>.

### 3.4. Oligomer formation and stoichiometry of the N-PLA<sub>2</sub>/LMW-heparin complex

Measurement of turbidity changes for N-PLA<sub>2</sub>/heparin mixtures at different heparin concentrations (data not shown) showed significant oligomerization of N-PLA<sub>2</sub>/heparin complexes for heparin chain lengths longer than an octasaccharide. The stoichiometric ratios of protein to carbohydrate in such complexes were assayed directly [17]. The ratios are seen to be 2.38, 1.93 and 1.85 for N-PLA<sub>2</sub>/LMW-heparin ratios of 10/8, 10/25 and 10/200, respectively. Thus heparin possibly has two N-PLA<sub>2</sub> binding sites and, on average, there are two N-PLA<sub>2</sub> molecules per heparin in the observed N-PLA<sub>2</sub>/LMW-heparin complexes.

### 3.5. Molecular docking of heparin with N-PLA<sub>2</sub>

Shown in Fig. 3 are the results of docking experiments on the computer between heparin and N-PLA<sub>2</sub>. The top panel of Fig. 3A provides the 3-D structure of the decasaccharide heparin molecule and the middle panel shows the stereo view of this heparin bound to N-PLA<sub>2</sub>. Most of the observed interactions occur between the positively charged cluster near the carboxy-terminus and the anionic sulfate residue of IdoA-8 and GlcN-9 (Fig. 3A). Specifically, the 2-N-SO<sub>3</sub><sup>−</sup> and 6-O-SO<sub>3</sub><sup>−</sup> of GlcN-9 can be seen to interact with Lys-114, 115 and Arg-116 of N-PLA<sub>2</sub> molecules, respectively (bottom panel

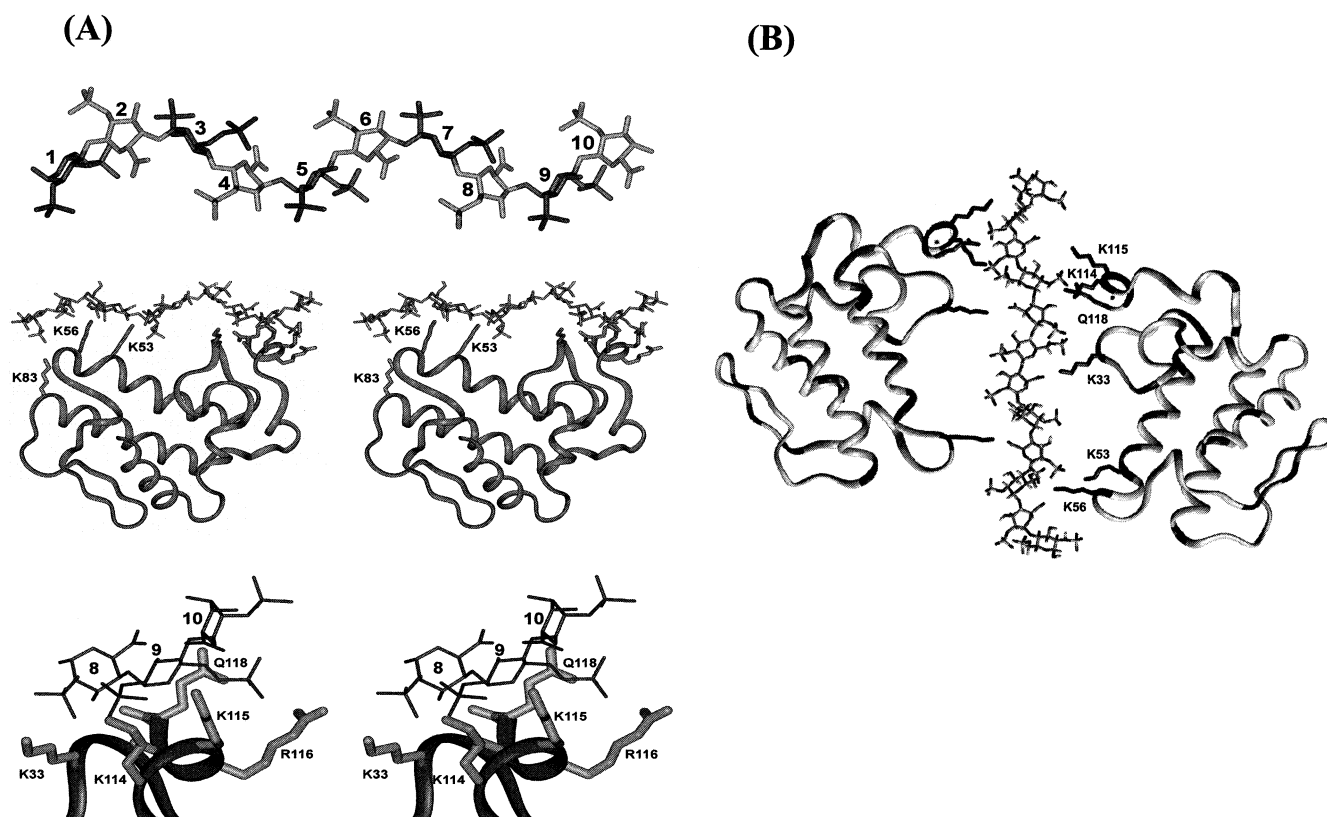


Fig. 3. Molecular model of the heparin/N-PLA<sub>2</sub> complex to explain the binding specificity (A) and stoichiometry (B) of the chain length-dependent interaction of heparin with N-PLA<sub>2</sub>. In the top panel of A, the three-dimensional structure of decasaccharide heparin molecule with iduronic acid (IdoA, labeled with even numbers) and glucosamine (GlcN, labeled with odd numbers) disaccharide repeats is illustrated. Stereodiagram of the molecular model of heparin/N-PLA<sub>2</sub> complex is shown in the middle panel. Close-up view of the complex with viewing direction aligned along the heparin chain is given in the bottom panel. Positively charged residues, other than those near the carboxy-terminus, involved in the heparin binding are labeled. B: Proposed model for the interaction of N-PLA<sub>2</sub> with the dodecasaccharide heparin to form the trans-dimer complex. All figures were prepared using the program RasMol V2.6.

of Fig. 3A). Nevertheless, consistent with our experimental data, several non-electrostatic hydrogen bond interactions can be found between the 3-OH of IdoA-8 and the last two amino acid residues in the carboxy-terminus. Lys-33, which is located far away from the identified positively charged clusters based on primary amino acid sequence, interacts strongly with 2-O-SO<sub>3</sub><sup>-</sup> of IdoA-8. The model depicted here consists of the important feature that a quasi-symmetric N-PLA<sub>2</sub> binding site is also available on the heparin molecule on the opposite side of the original binding site if its chain length is equal to or longer than a decasaccharide. This can be inferred from the optimally bound configuration of the dodecasaccharide chain with the N-PLA<sub>2</sub> molecules shown in Fig. 3B. The most probable form of the heparin/N-PLA<sub>2</sub> complex implied from this model is two N-PLA<sub>2</sub> bound to one heparin chain and this is consistent with the direct measurement of stoichiometry between heparin and N-PLA<sub>2</sub> in the observed complexes. The aggregation of these complexes is a possibility, when increased areas of hydrophobic regions of N-PLA<sub>2</sub> are exposed upon heparin's binding and this is perhaps what is indicated by the enhanced ANS fluorescence intensity following the initial binding of heparin with N-PLA<sub>2</sub> (Fig. 2A).

Thus, the data presented show that N-PLA<sub>2</sub> binds to heparin via its C-terminal region and a possible dimer complex is formed at a protein to carbohydrate ratio of 2:1. Although the possibility of electrostatic interactions in regions other

than the C-terminus is seen (between positively charged Lys-83, Lys-56, and negatively charged 6-O-SO<sub>3</sub><sup>-</sup> of GlcN-1 and 6-CO<sub>2</sub><sup>-</sup> of IdoA-2; Fig. 3B), the binding near the C-terminus depends on both electrostatic and non-electrostatic interactions. The binding seems to be specific to the amino acid sequence and the strength is dependent on the length of the heparin chain as well as the presence of *N*-sulfate groups on heparin. The formation of dimer complexes assumes significance when we note that the crystal structures of many snake venom PLA<sub>2</sub>s exhibit either a dimeric or a trimeric form with unknown biological activity [18].

**Acknowledgements:** This work was supported by the National Health Research Institute, Taiwan (Grant DOH88-HR-810).

## References

- [1] Dennis, E.A. (1997) Trends Biochem. Sci. 22, 1–2.
- [2] Hack, C.E., Wolbink, G., Schalkwijk, C., Speijer, H., Hermens, W.T. and van den Bosch, H. (1997) Immunol. Today 18, 111–115.
- [3] Kini, R.M. and Evans, H.J. (1989) Toxicon 27, 613–635.
- [4] Wu, W. (1998) Trends Cardiovasc. Med. 8, 270–278.
- [5] Dua, R. and Cho, W. (1994) Eur. J. Biochem. 221, 481–490.
- [6] Thompson, L.D., Pantoliano, M.W. and Springer, B.A. (1994) Biochemistry 33, 3831–3840.
- [7] Patel, H.V., Vyas, A.-A., Vyas, K.A., Liu, Y.-S., Chiang, C.-M., Chi, L.-M. and Wu, W. (1997) J. Biol. Chem. 272, 1484–1492.

- [8] Yang, C.-C., King, K. and Sun, T.-P. (1981) *Toxicon* 19, 645–659.
- [9] Joubert, F.J. (1977) *Biochim. Biophys. Acta* 493, 216–227.
- [10] Vyas, A.A., Pan, J.-J., Patel, H.V., Vyas, K.A., Chiang, C.-M., Hwang, J.-K. and Wu, W. (1997) *J. Biol. Chem.* 272, 9661–9670.
- [11] Beattie, K.L. and Foeler, R.F. (1991) *Nature* 352, 548–549.
- [12] Yamada, S., Murakami, T., Tsuda, H., Yoshida, K. and Sugahara, K. (1995) *J. Biol. Chem.* 270, 8696–8705.
- [13] Rice, K.G., Rottink, M.K. and Linhard, R.J. (1987) *Biochem. J.* 244, 515–522.
- [14] Mallis, L.M. (1989) *Anal. Chem.* 61, 1453–1458.
- [15] Yamada, S., Sakamoto, K., Tsuda, H., Yoshida, K., Sugiura, M. and Sugahara, K. (1999) *Biochemistry* 38, 838–847.
- [16] Scott, D.L., White, S.P., Otwinowski, Z., Yuan, W., Gelb, M.H. and Sigler, P.B. (1990) *Science* 250, 1541–1546.
- [17] Bock, P.E., Luscombe, M., Marshall, S.E., Pepper, D.S. and Holbrook, J.J. (1980) *Biochem. J.* 191, 769–776.
- [18] Segelke, B.W., Nguyen, D., Chee, R., Xuong, N.H. and Dennis, E.A. (1998) *J. Mol. Biol.* 279, 223–232.